Fabrication and Characterization of Three Dimensional Scaffolds for Tissue Engineering Application via Microstereolithography Technique

***Marina Talib, *James A Covington, **Andrew Dove, ***Aminat Bolarinwa, ***Liam Grover**

*School of Engineering, University of Warwick, **Department of Chemistry, University of Warwick, CV4 7AL UK, *** School of Chemical Engineering, University of Birmingham, Birmingham, B15 2TT, United Kingdom

Abstract

Microstereolithography is a method used for rapid prototyping of polymeric and ceramic components. This technique converts a computer-aided design (CAD) to a three dimensional (3D) model, and enables layer-per-layer fabrication curing a liquid resin with UV-light or laser source. However, the use of stereolithography in tissue engineering has not been significantly explored possibly due to the lack of commercially available implantable or biocompatible materials from the SL industry. This study seeks to develop a range of new bio-compatible/degradable materials that are compatible with a commercial 3D direct manufacture system (envisionTEC Desktop). Firstly, a selection of multifunctional polymer and calcium phosphate were studied in order to formulate biodegradable photopolymer resin for specific tissue engineering applications. A 3D structure was successfully fabricated from the formulated photocurable resins. The photopolymer of ceramic suspension was prepared with the addition of 50-70wt% of calcium pyrophosphate (CPP) and hydroxyapatite (HA). They were then sintered at high temperature for polymer removal, to obtain a ceramic of the desired porosity. Mechanical properties, morphology and calcium phosphate content of the sintered polymers were characterised and investigated with SEM and XRD, respectively. The addition of calcium phosphate coupled with high temperature sintering, had a significant effect on the mechanical properties exhibited by the bioceramic. The successful fabrication of novel bioceramic polymer composite with MSL technique offers the possibility of designing complex tissue scaffolds with optimum mechanical properties for specific tissue engineering applications.

Katakunci/keywords : Biomaterial,rapid prototyping, microstereolithography,calcium phosphate, tissue engineering

INTRODUCTION

Scaffolds are three dimensional supports that are use as a template at the site injury in guiding cell or tissue growth, regenerate and secret their own extracellular matrix in assisting the body in growing new, functional tissue. Scaffolds work in two ways, they either helping direct cell growth or simply providing a shape for the final tissue. A material that can be used as a scaffold in tissue engineering must satisfy a number of requirements. Important properties in this regard include biocompatibility and biodegradation; it should not elicit severe inflammatory responses, and it should degrade into non-toxic compounds within the time frame required as newly formed tissue is formed. The scaffolds should have suitable porosity for cell in-growth, a surface that balances hydrophilicity and hydrophobicity for cellular attachment, and mechanical properties that are compatible with those of the tissue as well as maintaining mechanical strength during most part of the tissue regeneration process. They can be formulated to contain additives or active agents for more rapid tissue growth or compatibility. For example, a bone implant may contain a form of calcium phosphate or a growth factor such as one of the bone morphogenetic proteins (Gunatillake & Adhikari 2003).

The fabrication of scaffolds for better tissue regeneration has attracted a great deal of attention. The fabrication of three-dimensional (3D) scaffolds that mimic the in vivo cellular microenvironment is fundamental importance to the success of tissue engineered constructs. Most scaffolds in tissue engineering have been fabricated by the traditional fabrication methods such as gas foaming/salt leaching (Nam et al. 2000; J. Yoon 2003), and freeze drying (O'Brien 2004; Fu et al. 2008). However, these methods do not control the inner/outer architecture, pores, porosity, and interconnectivity. Rapid prototyping technology has been utilised extensively because it has highest fabrication accuracy which could overcome some of the drawback of conventional methods.

Rapid Prototyping is a group of related technologies that uses computer-aided design (CAD) to create three-dimensional model (Drizo & Pegna 2006). These methods are unique in that they add and bond materials in layers to form objects. Such systems are also known as additive fabrication, three dimensional printing, solid freeform fabrication and layered manufacturing. The main highlight of these technologies are their capability to formed object with any geometric complexity or intricacy without the need for elaborate machine setup or final assembly and can be made from multiple materials, or as composites, or materials can even be varied in a controlled fashion at any location in an object. Among of the process falls under the field of rapid prototyping are

stereolithography apparatus (SLA), selective laser sintering (SLS), fused deposition modelling (FDM), laminated object manufacturing (LOM), and; inkjet-based systems and three dimensional printing (3DP).

Stereolithography generally is considered to provide the greatest accuracy and best surface finish of any rapid prototyping technology (Sun et al. 2005). It ability to produce a custom build in less time and cost found with casting methods, such as tooling and set-up. The technology is also notable for the large object sizes that are possible. Over the years, a wide range of materials with properties mimicking those of several engineering thermoplastics have been developed. Limited selectively colour changing materials for biomedical and other applications are available, and ceramic materials are currently being developed (Baroli, 2006; Leong et. al 2003; Yeong, Chua, Leong, & Chandrasekaran, 2004).

The use of stereolithography in tissue engineering has not been significantly explored, perhaps because of the lack of commercially available implantable or biocompatible materials from the SL industry. Polyethylene glycol (PEG) with an acrylates group is a suitable candidate for this kind of rapid prototyping technique. PEG has characteristic properties such as high hydrophilic, good tissue biocompatibility, lack of toxicity and availability of reactive sites for chemical modification whereas acrylates monomers are known for their high reactivity, polymerise rapidly in the present of photogenerated free radicals. It produced strong crosslinked bonds between acrylates groups and showed promising biocompatibility from cellular test.

MATERIALS AND METHODS

Synthesize and Preparation of Ceramic Suspension (CPP-A)

Calcium pyrophosphate (CPP-A) was synthesised at the School of Chemical Engineering, University of Birmingham (Bolarinwa et al. 2009). The brushite cement was synthesized by combining β tricalcium phosphate (β-TCP) with 3.5 M phosphoric acid (H_3PO_4) (Fisher Scientific, Dorset, UK) containing citric acid at a concentration of 50 mM (Fluka, Dorset, UK).The β-TCP was mixed with H_3PO_4 solution at powder to liquid ratio (P:L) of 1.25 g/mL. The resulting paste was cast into a polytetrafluroethylene (PTFE) split mould to form cylindrical samples of diameter 6 mm and height 12 mm.

The cylinders were allowed to harden at 37°C for 24 h prior to testing or further heat treatment. The hardened cement cylinders were subsequently sintered at temperatures between 400 and 1200°C for 5 h using a muffle furnace (CWF 1300; Carbolite, UK), the heating and cooling rate of the furnace was set at 10°C/min converting the brushite cement into monetite and then calcium pyrophosphate ceramic ($Ca_2P_2O_7$) in accordance with equation below:

$$\beta - Ca_3(PO_4)_2 + H_3PO_4 + 6\,H_2O \rightarrow 3CaHPO_4.2H_2O$$
$$2\,CaHPO_4.2H_2O \rightarrow 2\,CaHPO_4 + 4H_2O$$
$$2CaHPO_4 \rightarrow Ca_2P_2O_7 + H_2O$$

The hardened cylinders CPP were then crushed with a pestle and mortar into a powdery form. Upon crushing, the CPP's powder was then ball milled with Luckham, Multimix Major, [TM] for 24, 48 and 72 hours in order to get superfine particle size with less than 10 μm. Hydroxyapatite with the commercial name of CAPTAL ®S from Plasma Biotal Limited (CAPS), UK, were obtained and ball milled as well for comparison purposes.

Ceramic suspension

The photopolymer resin consists of precursor monomers; dipentaeryolacrylate and hexanediol ethoxylate diacrylate and Bisphenol A as reactive diluents. Polymer component of the suspension was prepared prior to mixing with the ceramic. The polymer, monomer and photoinnitiator were purchased from Sigma Aldrich, UK whilst the dye was from Kremer Pigmente, Germany.

Table 6.1 Optimum formulation of photo-curable polymer resin.

		Abbreviation	Ratio (%)
Monomer	Dipentaeryolacrylate	DPA	60*
Reactive diluents	Hexanediol ethoxylate diacrylate	HDeDA	30*
	Bisphenol A	BPA	10*
Photoinnitiator	2-benzyl-2-(dimethylamino)-4'-morpholino-butyrophenone	PI	3*
Dye	Orasol ® Orange G		0.5**

*: base on the weight of the polymer/monomer

**: base on the weight of the ceramic

The liquid components were mixed and stirred on a magnetic stirrer for 15 minutes. The percentage of the ceramics powder was varied from 50-150 wt% of polymer weight, where every 10 wt% of ceramic powders was added to the suspension every 15 minutes. 0.5 wt% of dye was added before leaving the suspension stirring for 24 hours. The photoinitiator was added and stirred for 1 hour prior to testing or used in the manufacturing process.

Ceramic discs of calcium phosphate (5 mm height x 4 mm diameter) were designed and fabricated via the Envision Desktop®. The compressive strength was measured with a universal testing machine (Instron 5569, Instron Corp., Canton, MA) with a crosshead speed of 0.1 mm/min. The compressive stress of the sintered ceramic (σc) can be calculated in accordance with equation:

$$\sigma_c = \frac{4F}{\mu d^2}$$

Where F is the load at failure (N) and d is the diameter of the ceramic sample (mm). In order to study the bioactivity, samples were soaked in simulated body fluid (SBF) [8] at body temperature (37 °C) and pH=7.4 for several periods. The SBF has a composition similar to human blood plasma and has been extensively used for in vitro bioactivity tests (Kokubo & Takadama 2006). For each period, the pH value of the sample was measured, with an Automatic Potential Titrator (China). Three samples were prepared for every scaffold and the reported pH was the average of three samples. After soaking, specimens were taken from the fluid, rinsed with deionised water, and dried at 37 ℃ for SEM connected with energy dispersive spectroscopy (SEM-EDAX), Model Zeiss Sigma, UK. The sintering temperature was maintain at 1250°C, but varied in the sintering time from 5-20 hours.

Heating profile

Room temperature 10°C/min 300°C (1 hr) 2°C/min 500°C (1hr) 2°C/min 1250°C RT1, RT2, RT3, RT4, RT5

where RT1, RT2, RT3, RT4 and RT5 was 5, 7, 10, 12, and 20 hours respectively.

Table 1 Composition of ceramic suspension photo-curable resin.

Calcium Phosphate	Weight % (wt%)[i]	Abbreviation	Photopolymer Resin	Ratio (%)[ii]
CPP-A	50	50A	*HDeDA	70
	70	70A	*DPA	20
	100	100A	*BPA	10
HAP	50	CAP50	PI	3[a]
	70	CAP 70	Dye	0.15[b]
	100	CAP 100		

[i] : weight percent of total weight of prepolymer (*)
[ii]: ratio based on total volume of prepolymer (*)
[a] : weight percent of PI based on the total weight of prepolymer (*)

RESULTS AND DISCUSSION

Effect of Sintering Time on Compressive Strength and Young's Modulus of Calcium Phosphate

Figure 1 shows a linear relationship between the true density and an increase sintering temperature. Changing the loading of the ceramic ratio also significantly affects the density as the sintering time increased. For instance, the density of the green body CPP-100A increases by 80% after sintering for 5 hours. In addition, increasing the sintering time from 5-20 hours also increases the density of CPP-100A to 45%.

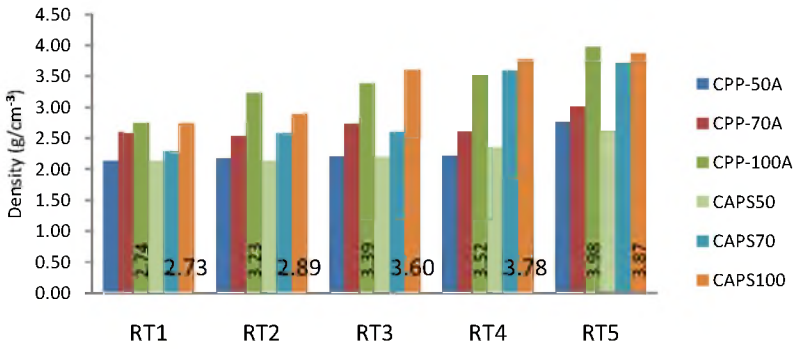

Figure 1 Density of different ratio of CPP-A, CPP-B and HAP for different heating profile.

Table 2 Effect of sintering time on the porosity of the ceramic composite

Sintering Time	Porosity (%)					
	CPP-A			HAPS		
	50	70	100	50	70	100
RT1 (5 hours)	47	48	51	22	18	23
RT2 (7hours)	49	51	53	25	27	28
RT3(10 hours)	55	56	61	31	29	33
RT4 (15 hours)	61	63	66	33	35	37
RT5 (20 hours	73	73	78	34	37	41

The porosity degree in Table 2 was quantified by GM methods and is reported as a function of the sintering time. The results show that with an increase in sintering time the ceramic porosity is increased. As the sintering time is increased, the necks formation becomes apparent as more particles become diffused to the neighbouring powder particles. The necks are then merges and shrink resulting in the change of grain shape and formation of interconnected pores along the particle junctions (Gbureck et al. 2008). The pores interconnectivity is well defined and consequently affects the microstructure of the composite (Figure 2). By increasing the sintering time from 5 to 20 hours, the grain size increases greatly to 7.99 µm from 5.52 µm whereas the density increases to 3.98 g/cm^{-3} from 2.74 g/cm^{-3} as shown in Figure 4. Grain growth can be expressed by equation (Brooks 1976):

$$G^a - G_o{}^a = K_o t \exp\left(-\frac{Q}{RT}\right)$$

where G and G_0 are the average grain size after and before sintering, a is the kinetic grain growth exponent, T is the sintering temperature, t is the sintering time, Q is the apparent activation energy for grain growth, K_o and R are constants. According to this grain-growth model, CPP grains have more time to grow for a longer sintering time. These results are coincide with the increases of average grain size and density of CPP with increase of the sintering time.

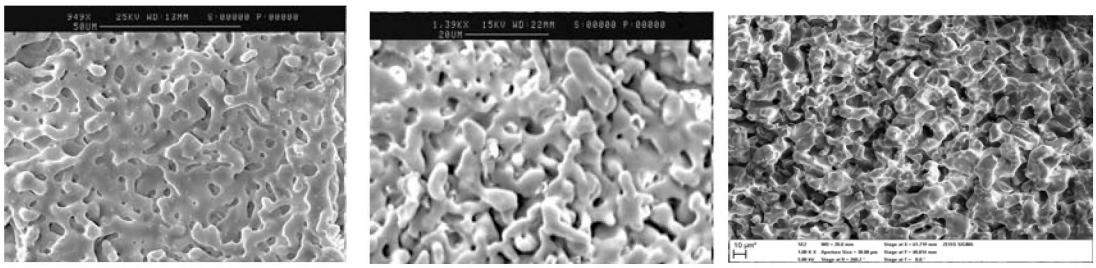

(a) (b) (c)

Figure 2 Surface morphology for CPP-A after sintering for (a) 5 hours, (b), 12 hours and (c) 20 hours (1000x magnification)

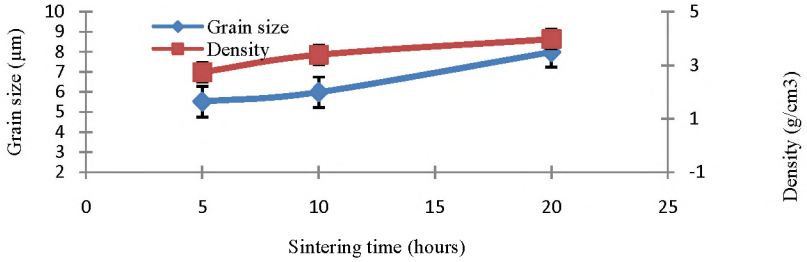

Figure 3. The grain size and density of CPP-A with different sintering times

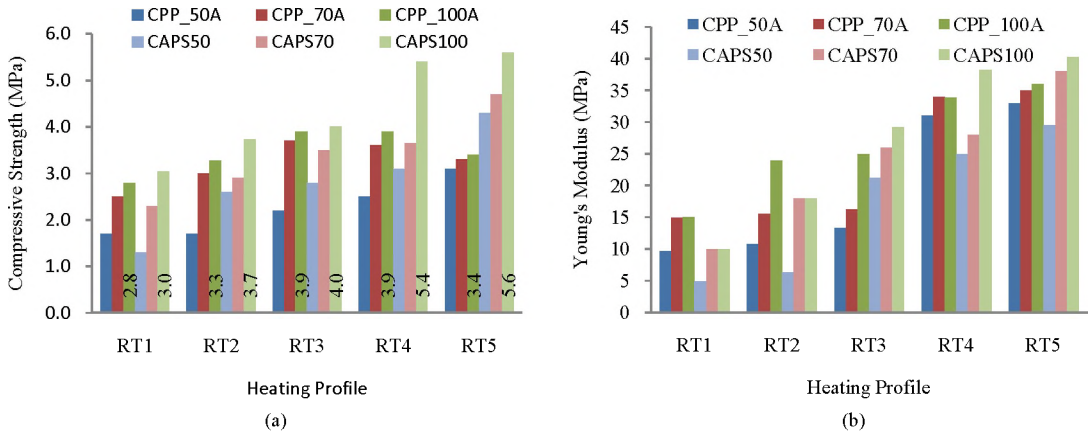

Figure 4. Effect of sintering time on the (a) compressive strength and (b) Young's modulus of different ratio of calcium phosphate ceramic composite.

The compressive strength and elastic modules were determined from the stress–strain relationship. Figure 4 shows the effect of increasing sintering time on the compressive strength and Young's modulus for various compositions of calcium phosphate. The compressive strength increases as the density increases, which is in agreement with the increase of density, as shown Figure 3. It can be observed that for CPP-100A, the true density increased from 24% when the sintering time increased from 5 to 20 hours. As a consequence, the compressive strength of CPP sintered for 20 hours is higher than that of samples sintered for 5 hours. The volumetric shrinkage could also be linked to the ceramic densification, which also could influence the compressive strength of the sintered ceramic.

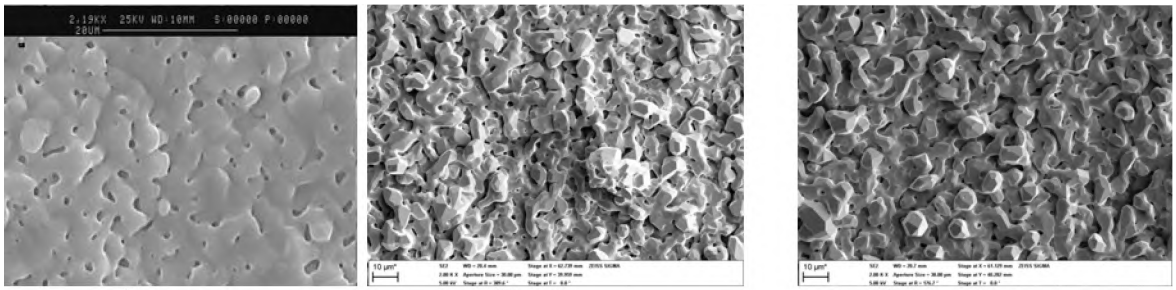

Figure 5. Surface morphology for polymer ceramic at different sintering time; (a) 5 hours, (b) 12 hours and (c) 20 hours prepared from HAP suspension.

The surface morphology of the polymer ceramic HAP, has shown the most apparent transformation as the sintering time increases from 5 hours to 20 hours (Figure 6). HAP is well known to have a higher surface energy. The high diffusion rate resulting from this high surface energy gives rise to better inter particle contact and increases the elastic modulus of the composite (Luo, J. AU - Stevens 1997). At 5 hours (Figure 5.(a)), the surface of HAP is mostly closed, with the surface shows rounding of particles and early stage neck formation. And as the time increases pore starting to interconnected and the angular-necking shape become highly visible. At 20 hours of sintering, the interconnected pores evolved to pore closure and further crystal densification which contributes to the increased of mechanical properties.

Any new biomaterial developed as a bone replacement should have mechanical strength similar to the natural bone, to maintain integrity until the new tissue regenerates. The compressive strength and Young's modulus of cancellous bone has been reported over a wide range between 4-12 and 20-500 MPa respectively (Karageorgiou & Kaplan 2005). In this study, the compressive strength of all CPP ceramic composite and HAP ranged from 1.7 MPa to 6.7 MPa and Young's modulus between 10 MPa and 45 MPa. The results suggest that it may be possible that different types of calcium phosphate could meet the mechanical requirements and support new bone tissue regeneration when implanted in the body, especially if the patient is not putting significant burden on the scaffold. Therefore in other to provide a clinical application for the formulated ceramic composite, a study on the vitro degradation of the composite was performed.

Bioactivity of Polymer Ceramic

SEM analysis demonstrates the strong influence of sintering time on the microstructure and morphology of the ceramic composites as discussed previously. It can be seen that the as the sintering time increases, the formation of microporosity becomes prominent and their connectivity offers good potential for cell attachment and proliferation. The variation of pH value relative to soaking times in simulated body fluid (SBF) of composite is shown in Figure 6.

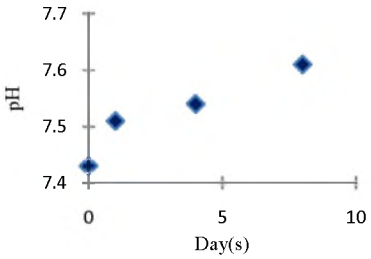

Figure 6. Variation of pH value in SBF for CPP-A

The increasing pH value during the first day is believed to be due to the partial dissolution at the surface level, indicating the high reactivity of these materials. These shows the interchange between Ca^{2+} and H_3O^+ during the formation of the apatite on bioceramics (Zhi-hua et al. 2006). These interchange increases the pH level, consequently encouraging the formation of apatite nuclei on the CPP and HAP surfaces. Figure 7 shows that the gradual development of apatite formation on the surface of CPP-70A for RT3 (sintering of 10 hours) as a result of increasing the number of days of immersion in SBF to 1, 4, and 8 days respectively.

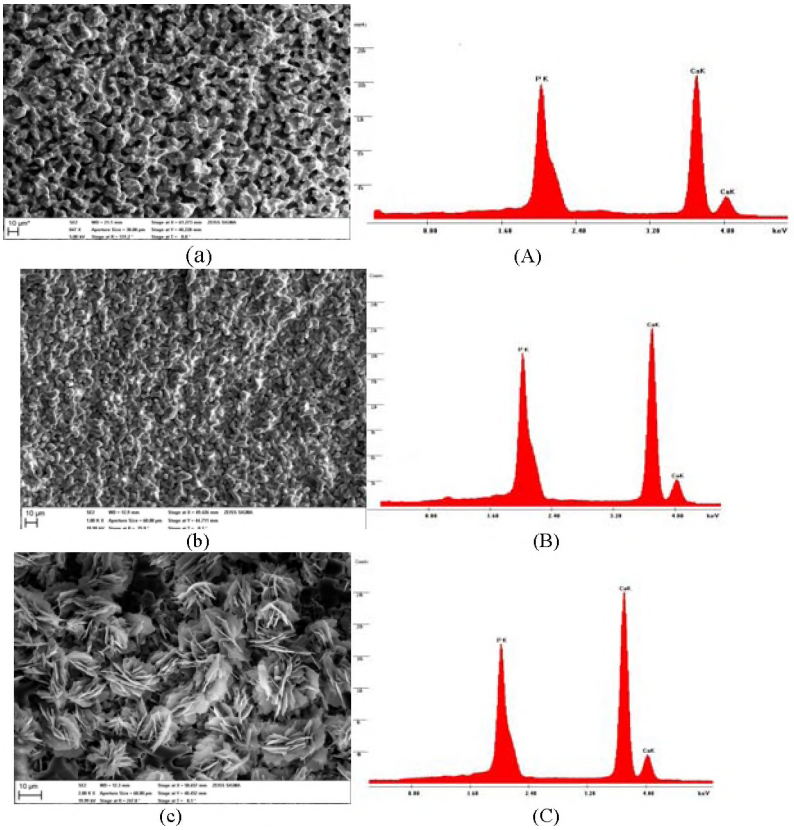

Figure 7 SEM micrograph of CPP-70A after soaking for (a) 1, (b) 4 and (c) 8 days. A, B and C represent their EDAX analysis respectively.

Figure 7 shows that as the soaking time increases, there were distinguishable changes on the surface morphology of the samples. After soaking the CPP-70A in SB for 8 days, there was an abundance of leaf-like depositions with lengths of 10 µm. These were evenly distributed over the surface of the samples, proving nucleation of apatite layer. The presence of large pores amongst the leaf-like crystallite indicates the effect of immersion and corrosion. The calculated Ca/P ratio is about 1.76 which is close to the theoretical value of

stoichiometric HA (Ca/P=1.67), and Ca/P ratio of the human bone, as it ranges between 1.6 and 1.7 depending on the age of the person.

Table 3 shows that the value of Ca/P ratio has increased from 1.20 before immersion to 1.30 after immersion confirming growth of apatite layer on the surface, which coincides with the EDAX analysis in Figure 8. The higher peak intensity of Ca after 8 days, explained the higher ratio Ca/P, as Ca ions are used for the re-precipitation process of HAP large particles (Bignon et al. 2002). On the other hand, the decrease in peak intensity of phosphorous, as shown in Figure 8 (A), (B) and (C), is believed to be due to the loss of phosphorous during sintering, as phosphorous could be escaping from the surface of the sample as gaseous oxides, when being sintered in air (Pattanayak et al. n.d.).

Table 3 Spectral calcium and phosphorous concentrations with their corresponding Ca/P ratios

Day	Sintering time					
	10 hr			20 hr		
	Ca (wt %)	P (wt %)	Ca/P	Ca (wt %)	P (wt %)	Ca/P
1st	57.14	42.86	1.33	52.89	47.11	1.12
4th	63.26	36.74	1.53	55.45	44.55	1.24
8th	64.81	35.19	1.76	57.43	42.57	1.31

Table 3 shows the spectrum of calcium and phosphorous concentrations, with their corresponding Ca/P ratios for 10 and 20 hours sintering time. This table shows that the Ca/P values for 20 hours are less when compare to 10 hours sintering time. The EDAX analysis has shown the low peak intensity of Ca and P, as shown in Figure 8(C). The small ratio of Ca/P has resulted in less formation of apatite on the composite surface. After 8 days in SBF medium, the apatite deposited on the surface of composite (RT5 CPP-70A) appeared as sub-micrometer crystals. The composite structure showed signs of immersion and corrosion, as were indicated by the reduction in pore size and shrinkage of composite surface area, as shown in Figure 8 (b).

The distinct difference of apatite formation, for both sintered times, could be seen in Figure 10(c) and Figure 10(b). As a comparison, the leaf-like particle formation on a 10 hour sintered sample, compared to the granule-like formation for a 20 hour sintered sample, shows the significant effect of sintering time on ceramic composite. By comparison, the surface morphology of RT5-CPP-70A (Figure 8 (b)) has similarities to RT3-CPP-70A (Figure 6(a)), which was immersed in SBF medium for 1 day. This suggest that for longer sintering times, the formation of apatite presumably only could occur if the immersion time was longer. Based on SEM and EDAX analysis on the composite samples, increasing the sintering time has a significant effect on the bioactivity of the samples, which contributes to the mechanical properties of each composites.

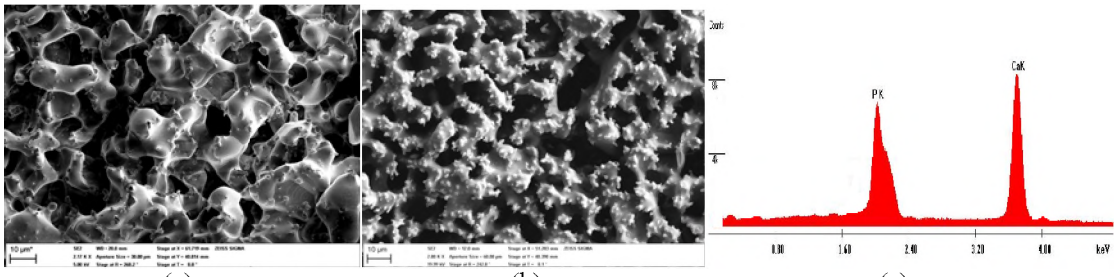

(a) (b) (c)

Figure 8 Surface morphology of RT5-CPP-70A for (a) pre-immersion and (b) post immersion and (c) EDAX analysis for post immersion of the composite sample after 8 days in SBF solution.

CONCLUSION

In this study it was shown that it was possible to synthesize a new photopolymer resin filled with calcium phosphate powder and to fabricate calcium pyrophosphate ceramics of defined architecture via a microstereolithography technique. Different sintering times were designed in order to study its effect on the mechanical properties and microstructure of the composites. With low sintering times of 5 to 10 hours, the compressive strength increases

significantly for both types of CPP as well as with increasing the CPP loading. However, further sintering time for 12 hour induced micro-cracks on the particles surface, which was responsible for decreasing the mechanical properties of the composites. Nevertheless, the compressive properties of the heat treated composite were quite close to those of cancellous bone (2–17 MPa).

In addition, XRD and SEM-EDAX confirmed the occurrence of apatite on the surface of ceramic composites. A study on sintering times has provided significant insight into the re-precipitation and microstructure of apatite formation, which coincided with the surface morphology shown in the SEM images. Increasing the sintering time was expected to enhance the apatite nucleation onto the composite surface. Finally, novel ceramic composites prepared from calcium phosphate have bioactivity properties that could be used in bone substitutes and tissue engineering applications.

REFERENCES

Baroli, B., 2006. Photopolymerization of biomaterials: issues and potentialities in drug delivery, tissue engineering, and cell encapsulation applications. *Journal of Chemical Technology & Biotechnology*, 81(4), pp.491-499.

Bignon, A., Chevalier, J. & Fantozzi, G., 2002. Effect of ball milling on the processing of bone substitutes with calcium phosphate powders. *Journal of biomedical materials research*, 63(5), pp.619-26.

Bolarinwa, a. et al., 2009. Cement casting of calcium pyrophosphate based bioceramics. *Advances in Applied Ceramics*, 109(5), pp.291-295.

Brooks, R.J., 1976. Treatise on Materials Science and Technology. In F. F. . Wang, ed. *Ceramic fabrication processes. Vol 9.* Academic Press, New York, p. 331.

Chen, A.A. et al., 2007. 3-D Fabrication Technology for Tissue Engineering. In pp. 23-38. Available at: http://dx.doi.org/10.1007/978-0-387-25844-7_2.

Drizo, A. & Pegna, J., 2006. Environmental impacts of rapid prototyping: An Overview of Research to Date. *Rapid prototyping Journal*, 12(2), pp.64-71.

Fu, Q. et al., 2008. Freeze-cast hydroxyapatite scaffolds for bone tissue engineering applications. *Biomedical materials (Bristol, England)*, 3(2), p.025005.

Gbureck, U. et al., 2008. Preparation of tricalcium phosphate/calcium pyrophosphate structures via rapid prototyping. *Journal of materials science. Materials in medicine*, 19(4), pp.1559-63.

Gunatillake, P. a & Adhikari, R., 2003. Biodegradable synthetic polymers for tissue engineering. *European cells & materials*, 5, pp.1-16; discussion 16.

Karageorgiou, V. & Kaplan, D., 2005. Porosity of 3D biomaterial scaffolds and osteogenesis. *Biomaterials*, 26(27), pp.5474-91.

Kokubo, T. & Takadama, H., 2006. How useful is SBF in predicting in vivo bone bioactivity? *Biomaterials*, 27(15), pp.2907-15.

Leong, K.F., Cheah, C.M. & Chua, C.K., 2003. Solid freeform fabrication of three-dimensional scaffolds for engineering replacement tissues and organs. *Biomaterials*, 24(13), pp.2363-2378.

Luo, J. AU - Stevens, R., 1997. The role of residual stress on the mechanical properties of Al2O3-5 vol% SiC nano-composites No Title. *Journal of the European Ceramic Society*, 17(13), p.1565.

Nam, Y.S., Yoon, J.J. & Park, T.G., 2000. A novel fabrication method of macroporous biodegradable polymer scaffolds using gas foaming salt as a porogen additive. *Journal of biomedical materials research*, 53(1), pp.1-7.

O'Brien, F., 2004. Influence of freezing rate on pore structure in freeze-dried collagen-GAG scaffolds. *Biomaterials*, 25(6), pp.1077-1086.

Pattanayak, D.K. et al., Synthesis and sintered properties evaluation of calcium phosphate ceramics ☆. *Engineering*.

Sun, C. et al., 2005. Projection micro-stereolithography using digital micro-mirror dynamic mask. *Sensors and Actuators A: Physical*, 121(1), pp.113-120.

Yeong, W.-Y. et al., 2004. Rapid prototyping in tissue engineering: challenges and potential. *Trends in biotechnology*, 22(12), pp.643-52.

Yoon, J., 2003. Dexamethasone-releasing biodegradable polymer scaffolds fabricated by a gas-foaming/salt-leaching method. *Biomaterials*, 24(13), pp.2323-2329.

Zhi-hua, Z. et al., 2006. Bioactivity of bioresorbable composite based on bioactive glass and. *Science*, (50174059).